Chapter 3
Fundamentals of Sliding-Mode Control Design

3.1 Introduction

This chapter provides an introduction to Variable Structure Control (VSC) theory and its extension to the so-called Sliding-Mode (SM) control. Note that the presentation is not intended as a comprehensive survey of the state-of-the-art in the field, but to merely supply the basic concepts on SM control required to understand the developments to come in this book. Readers well acquainted with this subject matter may omit this chapter. On the other hand, first-timers can use this material as a straightforward, but incomplete, introduction to the field of SM control, and are strongly encouraged to search for further and more substantial reading in the seminal works cited in the bibliography (useful introductory material could be, for instance, [5, 12, 14, 25, 26, 38, 44, 45]).

The chapter is divided in two parts. In the first one, Sect. 3.3, a general analysis of the classic or first-order SM control is formulated, which is the natural background to the subsequent generalisation known as Higher-Order Sliding-Mode control (HOSM). This section is mainly based on the influential works [38, 42, 44] and, to a lesser extent, on contributions from a series of classic survey papers such as [12, 45].

In the second part, Sects. 3.4 and 3.5, a general study of systems operating in sets of arbitrary sliding-mode order is presented. This section outlines the fundamentals of Higher-Order Sliding-Mode control theory, particularly focusing on Second-Order Sliding-Mode (SOSM) controllers. To a great extent, this part has been inspired in the works and results from [5, 25, 31, 33].

3.2 Variable Structure Control Preliminaries

The variable structure control and associated sliding modes were firstly proposed and developed by Stanislav Emelyanov and Vadim Utkin in the early 1950s in the Soviet Union [16, 43]. The most relevant feature of the SM control is its ability to

C. Kunusch et al., *Sliding-Mode Control of PEM Fuel Cells*,
Advances in Industrial Control,
DOI 10.1007/978-1-4471-2431-3_3,

generate robust control algorithms that are invariant under certain conditions. Briefly speaking, the concept of invariance indicates that the system remains completely insensitive to certain types of disturbances and uncertainties [13].

Since the 1990s, the control of systems subject to external disturbances and model uncertainty has been the focus of increasing interest. Among the different existing alternatives, the SM control has proven to be an attractive option to implement in systems electronically controlled, proving to be highly robust and even insensitive against certain system uncertainty and perturbations. The feasibility and benefits of SM control applied to electronically controlled actuators have been extensively demonstrated in the literature, such as [44]. In addition, the SM control allows a relatively simple design approach, even dealing with nonlinear systems, admitting a successful combination with other nonlinear control techniques such as energy shaping and model predictive control. As a result, the research and development of SM control design methods have been greatly accelerated, both in theoretical and practical fields [1, 6, 15, 36, 46].

One of the most distinctive aspects of the SM is the discontinuous nature of its control action. Its primary function consists in performing a switching between two different structures in order to get a desired new dynamics in the system, known as sliding-mode dynamics. This feature allows the system to have an enhanced performance, including insensitivity to parametric uncertainties and rejection to disturbances that verify the so-called *matching condition* [13, 38]. When the concept of parametric uncertainties is considered, it is referred to both external and internal uncertainties in the parameters as the product of the process of model reduction used in control design [14, 42].

However, a great deal of the success to fulfil the control objectives depends on the capability of the sliding-mode controller design to reduce *chattering*. The term chattering describes the phenomenon of finite-frequency, finite-amplitude oscillations appearing in many sliding-mode implementations. These oscillations are caused by the high-frequency switching of a sliding-mode controller under practical (non-ideal) operating conditions, such as unmodelled dynamics in the closed-loop or finite switching frequency [9, 22, 23, 44].

A successful alternative to reduce this undesired phenomenon, currently addressed by many control researchers and engineers, is to use the so-called Higher-Order Sliding-Mode control. In this case, from the definition of a continuous control action, the HOSM generalises the notion of sliding surface or manifold while keeping the main advantages of the original approach of SM for Lipschitz continuous uncertainty/perturbations. In particular, there are several promising results related to Second-Order Sliding-Mode control, existing several algorithms that solve the robust stabilisation of nonlinear uncertain systems, while guaranteeing a finite-time convergence of the sliding variable [5, 24, 29, 34].

3.3 Fundamentals of Sliding-Mode Control

The SM control is a strategy based on output feedback and a high-frequency switching control action which, in ideal conditions, is infinite. Essentially, this high-speed control law can lead the system trajectories to a subspace of the state space (commonly associated to a sliding surface or manifold). If a system is forced to constrain its evolution on a given manifold, the static relationships result in a dynamical behaviour determined by the design parameters and equations that define the surface [38]. On average, the controlled dynamics may be considered as ideally constrained to the surface while adopting all its desirable geometrical features.

Thus, making an appropriate design of the sliding surface (i.e. embedding the control objectives into the control function that gives rise to such manifold), it is possible to achieve conventional control goals such as global stability, optimisation, tracking, regulation, etc.

In the sequel, the basics of the theory of classical sliding-mode control are introduced, focusing on Single-Input Single-Output (SISO) systems. Note that in most sections of this chapter, the possible explicit dependence on time of the dynamical system has been omitted for the sake of clarity and economy of notation. In the present approach, this compacted notation can be used without loss of generality, provided that in the case of a non-autonomous system, it could be rewritten as autonomous by treating t as an additional dependent variable, with its trivial evolution given by the fictitious equation $\dot{t} = 1$ (obviously, at the expense of increasing the dimension by one).

3.3.1 Diffeomorphisms, Lie Derivative and Relative Degree

Firstly, it is useful to review some mathematical tools and procedures that will be necessary later. Let a control affine nonlinear system be given by

$$\begin{aligned} \dot{x} &= f(x) + g(x)u \\ y &= h(x) \end{aligned} \tag{3.1}$$

with $x \in X \subset \mathbb{R}^n$, $f : \mathbb{R}^n \to \mathbb{R}^n$ and $g : \mathbb{R}^n \to \mathbb{R}^n$ smooth vector fields (infinitely differentiable) with $g(x) \neq 0$, $h(x)$ smooth scalar field and $u : \mathbb{R}^n \to \mathbb{R}$ possibly discontinuous. These systems are linear in the control, so they are called control affine systems or analytical linear systems.

A diffeomorphism is defined as a coordinate transformation of the form $z = \phi(x)$ with $\phi : \mathbb{R}^n \to \mathbb{R}^n$ vector field with inverse ϕ^{-1}. In particular, we only consider transformations such that ϕ and ϕ^{-1} are $\mathscr{C}^n$ (i.e. with n continuous derivatives). This last condition ensures that the transformed system preserves the original system structure.

After making the proposed change of coordinates, the dynamical system (3.1) looks as follows:

$$\dot{z} = \dot{\phi}(x) = \frac{\partial \phi}{\partial x}\dot{x} = \frac{\partial \phi}{\partial x} f(x) + \frac{\partial \phi}{\partial x} g(x)u \tag{3.2}$$

Note that $\frac{\partial \phi}{\partial x} = [\frac{\partial \phi(x)}{\partial x_1} \, \frac{\partial \phi(x)}{\partial x_2} \cdots \frac{\partial \phi(x)}{\partial x_n}]$ gives the direction of the gradient vector of $\phi(x)$, $\nabla\phi(x)$. So the system (3.1) can be written in terms of the new variable z:

$$\begin{aligned} \dot{z} &= \tilde{f}(z) + \tilde{g}(z)u \\ y &= \tilde{h}(z) \end{aligned} \tag{3.3}$$

where

$$\begin{aligned} \tilde{f}(z) &= \frac{\partial \phi}{\partial x} f(x) \bigg\|_{x=\phi^{-1}(z)} \\ \tilde{g}(z) &= \frac{\partial \phi}{\partial x} g(x) \bigg\|_{x=\phi^{-1}(z)} \\ \tilde{h}(z) &= h(x)\|_{x=\phi^{-1}(z)} \end{aligned} \tag{3.4}$$

To simplify the notation, it is necessary to define the concept of directional derivative or *Lie derivative* [40], which is expressed as

$$(L_f h)(x) = L_f h(x) : \mathbb{R}^n \to \mathbb{R} \tag{3.5}$$

and represents the derivative of a scalar field $h(x) : \mathbb{R}^n \to \mathbb{R}$ in the direction of a vector field $f(x) : \mathbb{R}^n \to \mathbb{R}^n$,

$$L_f h(x) = \frac{\partial h}{\partial x} f(x) \tag{3.6}$$

L_f is a first-order differential operator, while the composition $L_f \circ L_g$, which is usually written as $L_f L_g$, is a second-order operator. Moreover, the directional derivative can be applied recursively:

$$L_f^k h(x) = \frac{\partial}{\partial x}\big(L_f^{k-1} h(x)\big) f(x) \tag{3.7}$$

In this way, a compact notation for the derivatives of scalar functions in the direction of vector fields is obtained. Either in the direction of a single vector field (f) or more (f and g):

$$L_g L_f h(x) = \frac{\partial}{\partial x}\big(L_f h(x)\big) g(x) \tag{3.8}$$

Finally, assuming a smooth output $h(x)$ of system (3.1), the relative degree of $h(x)$ at the vicinity of a given point x is defined as the smallest positive integer r, if one exists, with the property that

$$L_g L_f^i h = 0 \quad \forall 0 \le i \le r-2 \tag{3.9}$$

and

$$L_g L_f^{r-1} h \ne 0 \tag{3.10}$$

Therefore, a system output $h(x)$ with relative degree r implies, in a simplified way, that u explicitly appears for the first time at the rth time derivative of $h(x)$. In short, r gives an idea about how directly the control influences the output.

3.3.2 First-Order Sliding Mode

Consider the nonlinear dynamical system (3.1), with control action $u : \mathbb{R}^m \rightarrow \mathbb{R}$ (possibly discontinuous), f and g smooth vector fields with $g(x) \neq 0\ \forall x \in X$. Let s be defined as a smooth constraint function $s : X \rightarrow \mathbb{R}$, designed according to the desired control objectives (i.e. the specifications are fulfilled when s is constrained to zero), with gradient $\nabla s = \frac{\partial s}{\partial x}$ non-null on X [38]. Then the set

$$\mathscr{S} = \left\{x \in X \subset \mathbb{R}^n : s(x) = 0\right\} \tag{3.11}$$

defines a locally regular manifold in X (of dimension $n - 1$ in the case of a SISO system), called sliding manifold or, simply, switching surface. This order reduction feature is a characteristic of SM control systems (first and HOSM) and indicates that the subspace on which the sliding movements occur have "non-zero co-dimension", meaning that after reaching the sliding regime, the trajectories of the system will remain within a subspace of lower dimension than the space generated by n states. The results obtained below are of a local nature, restricted to an open neighbourhood of $X \subset \mathbb{R}^n$, having a non-empty intersection with the sliding manifold $\mathscr{S}$ [16, 28, 42].

In order to attain the sliding motion in such manifold, a variable structure control law can be proposed by imposing a discontinuous control action u, which takes one of two possible feedback values, depending on the sign of $s(x)$. For example,

$$u = \begin{cases} u^+(x) & \text{if } s(x) > 0 \\ u^-(x) & \text{if } s(x) < 0 \end{cases} \quad \text{with } u^+ \neq u^- \tag{3.12}$$

The upper and lower levels of u ($u^+(x)$ and $u^-(x)$, respectively) are smooth functions of x. Moreover, without loss of generality, it can be assumed that $u^+(x) > u^-(x)$ holds locally in X. Note that if $u^+(x) > u^-(x)$ for any point x, then the inequality holds for every x, given that the functions are smooth and do not intersect.

Suppose that, as a result of the control law (3.12), the constraint function locally satisfies the following inequalities in the neighbourhood of $\mathscr{S}$:

$$\begin{cases} \dot{s}(x) < 0 & \text{if } s(x) > 0 \\ \dot{s}(x) > 0 & \text{if } s(x) < 0 \end{cases} \tag{3.13}$$

Under these conditions, the system will reach the sliding manifold $\mathscr{S}$ and thereafter will remain confined in a vicinity of $\mathscr{S}$ (see Fig. 3.1). Then, it is considered that a sliding regime is established on $\mathscr{S}$ whenever (3.13) holds.

Using the notation of the directional derivative, $\dot{s}(x)$ can be expressed as follows:

$$\dot{s}(x) = L_{f+gu}s = L_f s + L_g s \cdot u \tag{3.14}$$

Note that the output $s(x)$ must have relative degree 1 with respect to u, i.e. $L_g s \neq 0$, to ensure that the discontinuous control action is able to influence the sign of $\dot{s}(x)$.

Expression (3.13) can also be written as follows:

$$\begin{cases} \lim\limits_{s \to +0} L_{f+gu^+}s < 0 \\ \lim\limits_{s \to -0} L_{f+gu^-}s > 0 \end{cases} \tag{3.15}$$

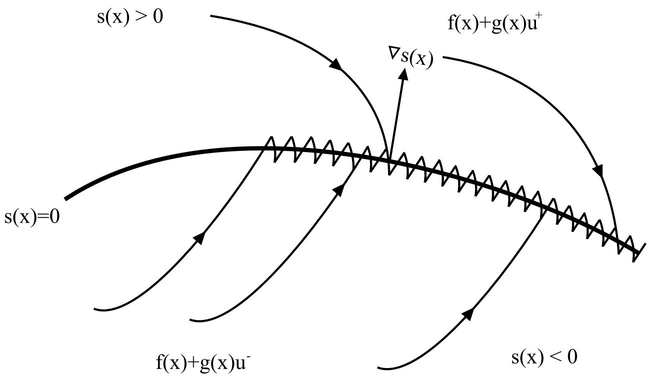

Fig. 3.1 Sliding manifold and system trajectories

meaning that the rate of change of the constraint or SM function $s(x)$, evaluated in the direction of the control field, is such that a crossing of the surface is guaranteed from each side of the surface, by using the switching law (3.12). This can be graphically interpreted with the help of Fig. 3.1, analysing the projection of the controlled field $f + gu$ onto the gradient vector ∇s at both sides of $\mathscr{S}$.

To conclude this subsection, a succinct final remark regarding the SM control finite reaching time is pertinent. Note then that the explicit condition (3.13) can be condensed as $\dot{s}(x)s(x) < 0$. From this it is simple to understand that, to achieve finite reaching time, the control law (3.12) must be designed to fulfil the previous inequality, but in a more strict way, that is according to the scalar sufficient condition $\dot{s}(x)s(x) < \kappa|s(x)|$ with $\kappa > 0$ (or, similarly, $\dot{s}(x)\,\mathrm{sign}\,s(x) < \kappa$). This means that the system should always be moving toward the switching surface with non-zero speed. This can be straightforwardly proven by taking $V = \frac{1}{2}s^2(x)$ as a Lyapunov function.

3.3.3 Equivalent Control Regularisation Method. Ideal Sliding Dynamics

From a methodological and systematic point of view, it is convenient to develop a regularisation method for deriving the sliding-mode equations for system (3.1). Assuming that the state vector is in the manifold $\mathscr{S}$ ($s(x) = 0$) and the sliding mode occurs with the state trajectories confined to this manifold for $t > 0$, one way to define the ideal sliding mode is using the so-called equivalent control method [44]. Since the motion in the sliding mode implies $s(x) = 0$ for $t > 0$, it may be assumed that $ds/dt = \dot{s} = 0$ as well. Hence, in addition to $s(x) = 0$, the time derivative $\dot{s}(x) = 0$ may be used to characterise the state trajectories during the sliding mode.

In summary, the equivalent control action is defined by the following invariance conditions on the switching manifold $\mathscr{S}$ [38]:

$$\begin{cases} s(x) = 0 \\ \dot{s}(x) = L_f s + L_g s \cdot u_{eq} = 0 \end{cases} \tag{3.16}$$

where $u_{eq}(x)$ is a smooth control law called *equivalent control* that makes $\mathscr{S}$ a local invariant manifold of system (3.1). Therefore, the equivalent control $u_{eq}(x)$ can be obtained from Eq. (3.16):

$$u_{eq}(x) = -\left.\frac{L_f s}{L_g s}\right|_{s(x)=0} \tag{3.17}$$

Thus, once $s = 0$ is attained, $u_{eq}(x)$ would provide the continuous control action required to maintain the system confined in the sliding surface.

The ideal sliding-mode dynamics, i.e. the closed-loop dynamics on the manifold $\mathscr{S}$, is obtained by substituting u_{eq} for u into (3.1):

$$\dot{x} = f(x) + g(x)u_{eq}|_{s(x)=0} = f(x) - g(x)\left.\frac{L_f s}{L_g s}\right|_{s(x)=0} \tag{3.18}$$

Note that the state variables are related by the algebraic equation $s(x) = 0$, reducing the order of the closed-loop system dynamics to $n - 1$.

Substituting the Lie derivative and operating in (3.18), we have

$$\dot{x} = \left[I - g\left(\frac{\partial s}{\partial x}g\right)^{-1}\frac{\partial s}{\partial x}\right]f(x) = \Psi(x)f(x) \tag{3.19}$$

Evaluated in $s(x) = 0$, (3.19) gives an idealised version of the motions occurring on the sliding manifold $\mathscr{S}$, constituting an "average" description of the trajectories of system (3.1) controlled with the VSC law (3.12).

The geometrical representation presented in Fig. 3.2 can be of help for a better understanding. In accordance with u_{eq} being the control action that makes the system remain on $\mathscr{S}$, the vector $\Psi f = f + gu_{eq}$ must lie in T_x, the tangent plane to $\mathscr{S}$ (i.e. normal to the gradient ∇s, as can be seen in Fig. 3.2). Mathematically this is expressed as

$$\Psi(x)f(x) \in \mathtt{ker}(\nabla s) \equiv T_x \tag{3.20}$$

Consequently, the matrix $\Psi(x)$ can be considered as a projection operator that, applied to the vector $f(x)$, projects it onto the plane tangent to surface $\mathscr{S}$ at the point x.

To conclude, it is of interest to briefly consider the effect of projector Ψ over any vector collinear with $g(x)$. Let Λ be a general vector of arbitrary amplitude, possibly a function of x, such that $\Lambda \in \mathrm{span}(g)$:

$$\Lambda(x) = g(x)\mu(x) \quad \text{with } \mu(x) : \mathbb{R}^n \to \mathbb{R} \tag{3.21}$$

Note then that the application of the operator $\Psi(x)$ to this vector projects Λ to the origin. In fact,

$$\Psi(x)\Lambda(x) = \left[I - g\left(\frac{\partial s}{\partial x}g\right)^{-1}\frac{\partial s}{\partial x}\right]g(x)\mu(x) = 0 \tag{3.22}$$

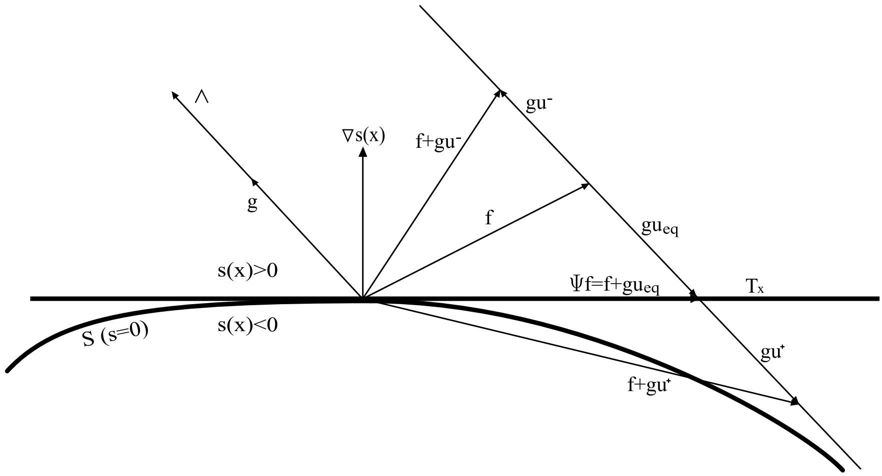

Fig. 3.2 Sliding surface and detail of the vector fields and projections

The cancellation of expression (3.22) can be interpreted in Fig. 3.2 as follows: the operator $\Psi(x)$ projects any vector in the direction of $g(x)$ onto the tangent subspace of $\mathscr{S}$. Hence, the projection of any vector that belongs to span(g) would result in just a point on T_x.

3.3.4 Existence Conditions for the First-Order Sliding Regime

3.3.4.1 Existence of Equivalent Control

It can be stated that the equivalent control is well defined if u_{eq} exists and is uniquely determined from the invariance conditions (3.16) [38].

Lemma 3.1 *The equivalent control is well defined if and only if the following condition is satisfied locally in* $\mathscr{S}$:

$$L_g s(x) = \frac{\partial s(x)}{\partial x} g(x) \neq 0 \tag{3.23}$$

This condition is known as "transversality condition" and may be inferred from (3.14). *The proof of the lemma can be found in* [38].

Geometrically, this lemma states that the vector field g cannot be tangential to the sliding manifold ($\mathscr{S} : g \notin \ker(\nabla s)$); otherwise it could not force the system to cross the surface. The transversality condition represents just a necessary condition for the existence of a first-order sliding mode.

3.3.4.2 Necessary Conditions for the Existence of a First-Order Sliding Regime

Based on the transversality condition, the following necessary condition for the existence of a sliding regime can be stated.

Lemma 3.2 *A necessary condition for the existence of a local sliding mode in* $\mathscr{S}$ *is that the equivalent control action* $u_{eq}(x)$ *must be well defined.*

Indeed, if u_{eq} is not well defined, i.e. $L_g s = 0$ at some point, the existence conditions of the sliding mode (3.15) cannot be satisfied simultaneously.

Lemma 3.3 *Assume, without loss of generality, that* $u^+(x) > u^-(x)$. *Then the following condition is necessary for the existence of a sliding regime on* $\mathscr{S}$:

$$L_g s(x) = \frac{\partial s}{\partial x} g(x) = \nabla s g(x) < 0 \tag{3.24}$$

The proof, direct from (3.15) and (3.16), is given in [38] and can be easily inferred from Fig. 3.2 by analysing the sign of the projection of $g(x)$ onto $\nabla s(x)$.

3.3.4.3 Necessary and Sufficient Condition for the Existence of a First-Order Sliding Regime

A necessary and sufficient condition for the local existence of a sliding mode in $\mathscr{S}$ is that, for $x \in \mathscr{S}$,

$$u^-(x) < u_{eq}(x) < u^+(x) \tag{3.25}$$

This condition can also be proved from (3.15) and (3.16) [38].

Then, u_{eq} can be interpreted as the averaged control signal resulting from the implementation of the maximum and minimum control actions, with an infinitesimal duty cycle resolution (in ideal sliding mode). However, in practice, several model imperfections and finite switching frequency make the state oscillate in a vicinity of the manifold [44].

3.3.4.4 Robustness of the First-Order SM

The behaviour of SM controlled systems under the effect of disturbances is discussed briefly. To this end, consider system (3.1) perturbed as follows:

$$\dot{x} = f(x) + g(x)u + \zeta(x) \tag{3.26}$$

with $\zeta(x)$ a vector of lumped perturbations that may take into account parametric perturbations of the nominal drift field or unstructured external disturbances

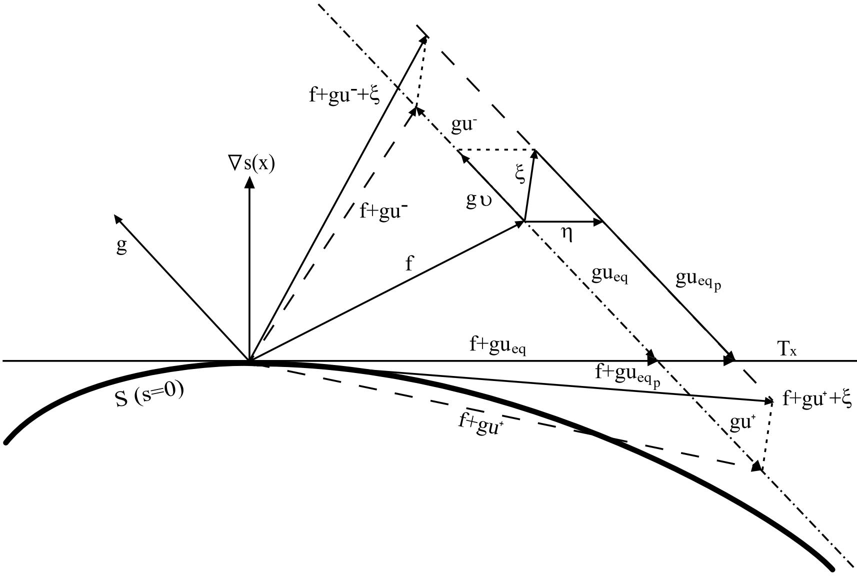

Fig. 3.3 Sliding surface and detail of the vector fields with perturbations

[38]. The vector $\zeta(x)$ can be uniquely decomposed into two components, one in the span(g), $g(x)\upsilon(x)$, and the other, $\eta(x)$, onto the tangent plane T_x (see Fig. 3.3):

$$\zeta(x) = g(x)\upsilon(x) + \eta(x) \tag{3.27}$$

It is said that the disturbances that belong to span(g) satisfy the matching condition, and the SM control is not merely robust to them but exhibits a strong invariance property. Effectively, as it can be observed in Fig. 3.3, if u^+ and u^- are strong enough, the component $g(x)\upsilon(x)$ can be completely annihilated by the control, simply generating a new infinitesimal duty cycle and, consequently, a new equivalent control for the disturbed system ($u_{eq_p}(x) = u_{eq}(x) - \upsilon(x)$). In addition, the undisturbed or nominal sliding dynamics suffers no modifications.

On the other hand, it can be appreciated (in Fig. 3.3) that the tangential component of the disturbances, $\eta(x)$, cannot be rejected. However, it does not compromise the local existence of the sliding motion, but definitely influences the ideal sliding dynamics.

In accordance with this analysis, it can be stated that a necessary and sufficient condition for the local existence of a sliding mode in the perturbed system is

$$u^-(x) < u_{eq_p}(x) = u_{eq}(x) - \upsilon(x) < u^+(x) \tag{3.28}$$

A detailed demonstration is provided in [38].

3.3.5 Extension to Nonlinear Systems Non-affine in Control

Consider a generic system described by the following differential equation:

$$\dot{x} = F(x, u) \tag{3.29}$$

Using the same SM function $s(x)$, the controlled system can be again decomposed into two subsystems or structures, depending on whether $s(x) > 0$ or $s(x) < 0$:

$$\dot{x} = F(x, u) = \begin{cases} F(x, u^+) = F^+ & \text{if } s(x) > 0 \\ F(x, u^-) = F^- & \text{if } s(x) < 0 \end{cases} \tag{3.30}$$

Along the trajectories of the system, the dynamics of $s(x)$ has the following expression:

$$\dot{s}(x) = \frac{\partial s}{\partial x_1}\dot{x}_1 + \frac{\partial s}{\partial x_2}\dot{x}_2 + \cdots = \begin{bmatrix} \frac{\partial s}{\partial x_1} \frac{\partial s}{\partial x_2} \cdots \end{bmatrix} \begin{bmatrix} \dot{x}_1 \\ \dot{x}_2 \\ \vdots \end{bmatrix} = L_F s(x) \tag{3.31}$$

In the same way as in system (3.30), in the time derivative of the SM function two cases can be distinguished:

$$\begin{aligned} &\text{if } s > 0 \rightarrow \dot{s} = L_{F^+} s(x) \\ &\text{if } s < 0 \rightarrow \dot{s} = L_{F^-} s(x) \end{aligned} \tag{3.32}$$

As the trajectory has to converge to the manifold, when $s(x) > 0$, the states should move towards $s(x) = 0$ (i.e. $\dot{s}(x) < 0$, so $s(x)$ decreases), and conversely in the reciprocal case. This means that the establishment of the sliding mode on $s(x) = 0$ is fulfilled with a condition similar to (3.13):

$$\begin{aligned} &\text{if } s > 0 \rightarrow \dot{s} = L_{F^+} s(x) < 0 \\ &\text{if } s < 0 \rightarrow \dot{s} = L_{F^-} s(x) > 0 \end{aligned} \tag{3.33}$$

3.3.6 Filippov Regularisation Method

Besides the equivalent control method presented in Sect. 3.3, at this point it is of interest to introduce another regularisation method, also capable of dealing with discontinuous systems. In particular, the underlying concept behind this method will be of use in the higher-order SM control strategies to come.

Recall that conventional theory of differential equations is limited to continuous state functions, hence when dealing with discontinuous systems, it does not answer even fundamental questions, such as the existence and uniqueness of the solution. Strictly speaking, most conventional methods require the right-hand side of the differential equation (3.29) to satisfy the Lipschitz condition

$$\left\| F(x_1) - F(x_2) \right\| < L \|x_1 - x_2\| \tag{3.34}$$

Fig. 3.4 Hysteresis of the switching device

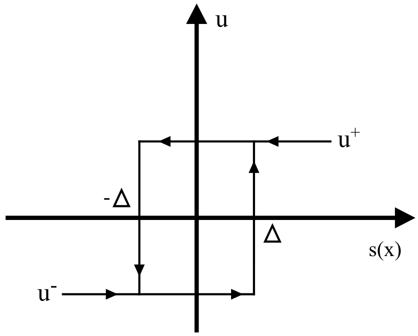

with L being some positive value, known as Lipschitz constant, for any x_1 and x_2. This condition implies that the function does not grow faster than some linear function [44]. Nevertheless, this is not the case for discontinuous functions if x_1 and x_2 are close to a discontinuity point.

So as previously stated, in situations where conventional methods are not applicable, the common approach is to employ different methods of regularisation like the equivalent control method proposed in [42]. Another useful regularisation method usually applied to general nonlinear systems as (3.29) is the so-called Filippov method [20]. This procedure consists of considering that the discontinuous control is implemented with a switching device with small imperfections. In particular, if a hysteresis loop of width 2Δ is considered, then the state trajectories oscillate in a Δ-vicinity of the switching surface when the control takes one of the two extreme values, $u^+(x)$ or $u^-(x)$ (see Fig. 3.4).

Δ is considered small enough, so the state velocities $F^+ = F(x, u^+)$ and $F^- = F(x, u^-)$ are assumed to be constant for some point x on the surface $s(x) = 0$ within a short time interval $[t, t + \Delta t]$. Let the time interval Δt consist of two sets of intervals Δt_1 and Δt_2 such that $\Delta t = \Delta t_1 + \Delta t_2$, $u = u^+$ during Δt_1 and $u = u^-$ during Δt_2. Then, the increment of the state vector once Δt is elapsed is found as

$$\Delta x = F^+ \Delta t_1 + F^- \Delta t_2 \tag{3.35}$$

and the average velocity of the state vector is given by the convex average of the velocity vectors:

$$\bar{\dot{x}} = \frac{\Delta x}{\Delta t} = \mu F^+ + (1 - \mu) F^- \tag{3.36}$$

where the convex average factor $\mu = \Delta t_1 / \Delta t$ can be understood as the percentage of time that the control takes the value u^+, while $(1 - \mu)$ is the percentage corresponding to u^-, with μ belonging to the closed set [0, 1]. Now, the procedure to get the state vector movement $\dot{x}$ is to make Δt tend to zero. Nevertheless, this limit is intrinsic to the assumption that the state velocity vector, or equivalently the vector field $F(x)$, is constant within the time interval Δt. Then, for the Filippov regularisation method, the convex expression

$$\dot{x} = \mu F^+ + (1 - \mu) F^- \tag{3.37}$$

Fig. 3.5 Filippov's regularisation method

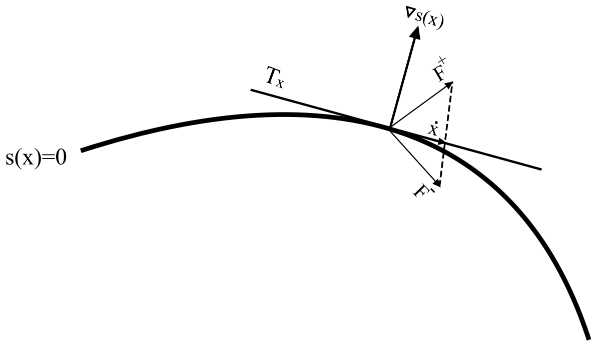

represents the motion during the first-order sliding mode (see the convex closure in Fig. 3.5, as a graphical interpretation of the Filippov method). Accordingly, since the trajectories during the sliding mode are on the manifold $s(x) = 0$, the following equation holds:

$$\dot{s} = \nabla s(x)\dot{x} = \nabla s(x)\left[\mu F^{+} + (1-\mu)F^{-}\right] = 0 \tag{3.38}$$

so the parameter μ should take a value that allows the state velocity of the system (3.37) to lie on the tangent plane (see Fig. 3.5). From (3.38) it can be easily inferred that such value of μ must be

$$\mu = \frac{\nabla s(x)F^{-}}{\nabla s(x)[F^{-} - F^{+}]}. \tag{3.39}$$

Note For control affine systems, the resultant sliding equations derived from the Filippov regularisation method are the same as those obtained from the Utkin equivalent control.

3.3.7 Discontinuous Control Action in Classic Sliding-Mode Control. Chattering Problem

One of the main drawbacks of the first-order sliding-mode control in certain applications is the direct use of discontinuous control actions. In actual implementations, the discontinuous control law, together with unmodelled dynamics and finite switching frequency, may produce fast oscillations in the outputs of the system. This effect is known as "chattering" phenomenon.

During the mid-1980s, the following three main approaches to reduce chattering in sliding-mode controlled systems were proposed [8]:

- The use of a saturation control instead of the discontinuous action [10, 39]. This well-established approach allows the control to be continuous, restraining the system dynamics not strictly onto the sliding manifold, but within a thin boundary layer of the manifold. This method ensures the convergence to the boundary layer, whose size is defined by the slope of the saturation linear region.

- The observer-based approach [9, 44]. This method allows bypassing the plant dynamics by the chattering loop. This approach successfully reduces the problem of robust control to the problem of exact robust estimation. However, in some applications it can be sensitive to the plant uncertainties, due to the mismatch between the observer and plant dynamics [45].
- The Higher-Order Sliding-Mode approach (HOSM) [18, 29]. This method allows the finite-time convergence of the sliding variable and its derivatives. This approach was actively developed since the 1990s [2, 4, 5, 29, 32, 37], not only providing chattering attenuation, but also robust control of plants of relative degree one and higher. Theoretically, an r*-order* sliding mode would totally suppress the chattering phenomenon in the model of the system (but not in the actual system) when the relative degree of the model of the plant (including actuators and sensors) is r. Yet, no model can fully account for parasitic dynamics, and, consequently, the chattering effect cannot be totally avoided. Nevertheless, theoretical results in HOSM, especially Second-Order Sliding-Mode algorithms, have been successfully proven in practice, encouraging the progress of the research activities.

Then, it is of natural interest the study of sliding-mode control alternatives that, smoothing the control action, reduce the chattering effects and avoid unnecessary requirements on the actuators. This is particularly relevant in fuel cell control, as there are mechanical actuators involved that may suffer when exposed to control actions of high frequency and amplitude.

It should be noted that when using Higher-Order Sliding Modes, it is not possible to maintain the invariance properties against matched disturbances as in the original approach. However, different control schemes that guarantee robust stability of the system can be achieved, satisfying the condition $s(x) = 0$ (and even zeroing higher-order derivatives of $s(x)$) in finite time [18, 25].

In the sequel, a brief introduction to Higher-Order Sliding-Mode control applied to uncertain nonlinear systems is presented. Then, Second-Order Sliding-Mode control and in particular three different algorithms are analysed in detail.

3.4 Some General Concepts on Higher-Order Sliding Modes

As discussed in Sect. 3.2, first-order sliding-mode control has certain properties that make it particularly attractive to apply to uncertain nonlinear systems. Among them, it can be highlighted finite convergence to the surface, system order reduction and robustness against certain disturbances. In this context, Higher-Order Sliding-Mode control will inherit some of these properties. This control approach generalises the idea of first-order sliding mode, by acting on the higher-order derivatives of the constraint function $s(x)$, instead of influencing the first derivative (as in (3.14)). Keeping the main advantages of the original approach, the HOSM control works with continuous action over $\dot{s}(x)$, relegating the discontinuous control to operate on the higher derivatives of $s(x)$. This weakens the effect of chattering in the output, providing greater accuracy in realisation. Additionally, in some applications (namely, plants with relative degree 1 with respect to s), the resultant physical control input to the plant is continuous, contributing to the longer service life of certain actuators. A significant number of these controller proposals can be found in [2, 7, 18, 21, 25, 29, 30, 35].

An important concept in HOSM is the notion of sliding order. If the goal is to maintain a constraint given by $s(x) = 0$, the sliding order is defined as the number of continuous time derivatives of $s(x)$ (including the zero-order one) in the vicinity of a sliding point. With these considerations, a sliding mode of order r is determined by the following equalities:

$$s = \dot{s} = \ddot{s} = \cdots = s^{(r-1)} = 0 \tag{3.40}$$

Expression (3.40) represents an *r-dimensional* condition in the dynamic system, which implies an order reduction of r (that is, (3.40) specifies r algebraic equations that bond the state variables).

3.4.1 Definition of Differential Inclusion

As in first-order sliding-mode control, the HOSM scheme forces a movement on a set of discontinuity, demanding an approach to the problem capable to deal with differential equations with right-hand side single-valued, but discontinuous, functions. Such an approach can be found in the Filippov concepts introduced in Sect. 3.3.6. The basic idea behind Filippov's method was not to focus on the value of the vector function precisely at the discontinuity point, but on its values in the point's immediate neighbourhood. Then, the function at the point is replaced with an average function, taken from a set generated by the convex combination of the values at each side of the discontinuity point.

This replacement can be interpreted as including or covering the discontinuous right-hand side single-valued function with a more comprehensive set-valued function (as would be the convex closure presented in the case treated in Sect. 3.3.6). This idea of inclusion, or better expressed differential inclusion, will be of help when designing SOSM controllers for dynamical system with uncertainties.

To better formalise this mathematical concept, consider a general differential equation of the form

$$\dot{z} = v(z, t) \tag{3.41}$$

where the generic variable $z \in \mathbb{R}^n$, and $v(z, t)$ is a piecewise-continuous single-valued function in a domain G with some points of discontinuity in a set M of measure zero. Note that in the framework of the SM control problem the generic variable z could be particularised to be a suitable variable of the dynamical system under control (for instance, x or, through a diffeomorphism, s, $\dot{s}$ and any appropriate internal variables), while the discontinuity set M could be the sliding manifold.

Next, for each point (z, t) of the domain G, a set-valued function $\mathscr{V}(z, t)$ in an n-dimensional space must be considered. Note that just as the single-valued function takes a point in its domain into a single point (direction) in another space, the set-valued function take a point in its domain into a set of points (directions) in another space [11]. In this particular case, for points (z, t) where function $v(z, t)$ is continuous, the set $\mathscr{V}(z, t)$ trivially consists of one point (direction) which coincides with the single value of $v(z, t)$ at this point. On the other hand, if (z, t) is a point of discontinuity of function $v(z, t)$, then $\mathscr{V}(z, t)$ comprises a set of directions rather than a single specific one. Now, in accordance with Filippov's definition, the discontinuous differential equation (3.41), can be formally replaced by an equivalent differential inclusion of the form

$$\dot{z} \in \mathscr{V}(z, t) \tag{3.42}$$

The expression above, is called a Filippov differential inclusion if the set $\mathscr{V}(z, t)$ is non-empty, closed, convex, locally bounded and upper-semicontinuous. In this way, $\mathscr{V}(z, t)$ can cover the situation in which the state derivative belongs to a set of directions, not to a single one. In the simplest case, i.e. when $v(z, t)$ is continuous almost everywhere, $\mathscr{V}(z, t)$ is the convex closure of the set of all possible limits of $v(t, z_{cont})$ as $z_{cont} \to z$, while z_{cont} are continuity points of $v(z, t)$.

Note that this definition verifies the description of $\mathscr{V}(z, t)$ previously given. When z_{cont} approaches a continuity point, the limits converge to a single value, so, as expected, $\mathscr{V}(z, t)$ effectively coincides with the continuous value of $v(z, t)$. Conversely, when z_{cont} approaches a discontinuity point, limits are different, and $\mathscr{V}(z, t)$ comprises a set of directions.

It can be stated, then, that a solution $z(t)$ of the differential equation (3.41) is understood as a solution in the Filippov sense, if it is an absolute continuous function in an interval and satisfies the differential inclusion (3.42) almost everywhere on such interval [19, 20].

Summarising, the Filippov definition replaces the discontinuous differential equation (3.41) by the differential inclusion (3.42). Removing sets of zero measure (discontinuity points) from the values taken by $v(z, t)$ corresponds to purposely ignoring possible misbehaviour of the right-hand side in (3.41) on small sets.

3.4.2 Sliding Modes on Manifolds

The notion of sliding mode manifold acquired with the first-order SM can be extended to HOSM. The progression that generates the successive sliding manifolds can be described as follows. Let $\mathscr{S}$ be the smooth manifold defined from a smooth function $s(x)$ (see Eq. (3.11)). The set of points x for which the set of possible velocities entirely lies in the subspace T_x tangent to $\mathscr{S}$ is defined as a second-order sliding set with respect to $\mathscr{S}$ (recall that in a first-order SM the set of possible velocities of the system does not lie in T_x, but intersects it. See Fig. 3.2). The former concept means that once $\mathscr{S}$ is reached, the Filippov solutions of Eq. (3.41) fall within the tangent space of the manifold $\mathscr{S}$. This set of points is denoted as $\mathscr{S}_2$. Assuming that $\mathscr{S}_2$ can be considered as a manifold smooth enough, the same construction can be performed for $\mathscr{S}_2$, calling $\mathscr{S}_3$ to the corresponding set of second-order sliding solutions with respect to $\mathscr{S}_2$ or third-order sliding set with respect to $\mathscr{S}$. Thus, continuing this way, one can find sliding sets of any order [25]. Summarising, it is said that there is an rth-order sliding mode on the manifold $\mathscr{S}$ in a neighbourhood of an rth-order sliding point $x \in \mathscr{S}_r$ if in a neighbourhood of this point x, the set $\mathscr{S}_r$ is an integral set, and this means that the set of trajectories is understood in the Filippov sense.

3.4.3 Sliding Modes and Constraint Functions. Regularity Condition

3.4.3.1 Definition of Regularity Condition

At this point, it is useful to briefly introduce the definition of the regularity condition and its relation with other concepts, such as the normal form of nonlinear systems. Hence, reconsider the constraint given by $s(x) = 0$, where $s : \mathbb{R}^n \to \mathbb{R}$ is a function smooth enough. Assume also that the time derivatives of $s(x)$, i.e. $\dot{s}, \ddot{s}, \ldots, s^{(r-1)}$ exist and are single-valued functions of x (which is not trivial in discontinuous dynamical systems). Recall that the discontinuity does not appear in the first $r - 1$ derivatives of the constraint function s, or analogously, s is an output of relative degree r with respect to the discontinuous input, according with (3.9) and (3.10). When these assumptions hold, the sliding set of order r will be unequivocally determined by Eqs. (3.40), implying that the reduced system dynamics has order $n - r$.

Definition 3.1 Consider the non-empty rth-order sliding set (3.40) and assume that it is a set locally integrable in the sense of Filippov (i.e. consisting of Filippov trajectories of the discontinuous dynamical system). Then, the corresponding motion that satisfies (3.40) is called rth-order sliding mode with respect to the constraint function s.

To show the relationship of this definition with other control definitions, consider a manifold $\mathscr{S}$ given by the equation $s(x) = 0$. Suppose that $s, \dot{s}, \ddot{s}, \ldots, s^{(r-1)}$ are smooth functions of x and

$$\operatorname{rank}\left\{\nabla s, \nabla \dot{s}, \nabla \ddot{s}, \ldots, \nabla s^{(r-1)}\right\} = r \tag{3.43}$$

holds locally. Then, since all $\mathscr{S}_i$, $i = 1, \ldots, r - 1$, are smooth manifolds, $\mathscr{S}_r$ is a differentiable manifold determined by (3.40). Recall that the rank of a set of vectors indicates the dimension of the subspace they define.

Equation (3.43), together with the requirement that the corresponding time derivatives of s are smooth functions of x, is referred to as the "*sliding regularity condition*" [25, 31].

This is a useful definition because if condition (3.43) is reached, new local coordinates $y_1 = s$ can be taken, and the system can be described through the following set of equations:

$$\begin{cases} \dot{y}_1 = y_2 \\ \dot{y}_2 = y_3 \\ \vdots \\ \dot{y}_r = \Phi(y, \xi) \\ \dot{\xi} = \Psi(y, \xi) \quad \text{with } \xi \in \mathbb{R}^{n-r} \end{cases} \tag{3.44}$$

Note that this is similar to the *normal form* of nonlinear systems; the only difference is that in the *normal* form $\dot{y}_r = a(y) + b(y)u$ [31].

Additional Remark It is sometimes mentioned that the higher-order sliding modes differ depending on the number of total derivatives of s which are extinguished when reaching the manifold $\mathscr{S}$. However, this number cannot be considered as a feature of the HOSM, since formally all orders of derivatives are cancelled at $\mathscr{S}$ [4]. The most important feature of a sliding mode is the number of successive *continuous* derivatives of s in the neighbourhood of the manifold. In other words, the value of r is taken from computing the first discontinuous or non-existent time derivative of s. The sliding order r is understood in this sense.

3.4.3.2 Connection with Other Well-Known Results in Control Theory

Let the control affine nonlinear system (3.1) be recalled as

$$\begin{cases} \dot{x} = f(x) + g(x)u \\ s = s(x) \in \mathbb{R} \\ u \in \mathbb{R} \end{cases} \tag{3.45}$$

with f, g and s sufficiently smooth vector functions.

Assuming that the output $s(x)$ has relative degree r, according to (3.9) and (3.10), this means that in the neighbourhood of a given point,

$$L_g s = L_g L_f s = \cdots = L_g L_f^{r-2} s = 0; \qquad L_g L_f^{r-1} s \neq 0 \tag{3.46}$$

hence $s^{(i)} = L^i_f s$ for $i = 1, \ldots, r-1$, and the regularity condition (3.43) is automatically satisfied. For this reason, a direct analogy between the *relative degree* notion and the *regularity condition of sliding mode* can be established. In general terms, it can be stated that the regularity condition (3.43) means that the relative degree of system output with respect to the discontinuity is at least r. Similarly, the notion of rth-order sliding-mode dynamics is analogous to the zero dynamics concept defined in [27]. The nominal stability of the controlled system can be guaranteed if the stability of (3.44) holds when $y = 0$, i.e. when the reduced system $\dot{\xi} = \Psi(y, \xi)$ with $\xi \in \mathbb{R}^{n-r}$ is stable.

3.4.4 Closing Comments on Higher-Order Sliding Modes in Control Systems

3.4.4.1 An Observation Regarding the Accuracy of Real Sliding Modes

It is necessary to clarify that when referring to a system operating in sliding mode, it can be both ideal (nominal) sliding, which takes place when the switching imperfections are neglected and the restriction is maintained accurately, or real sliding, which occurs when the switching imperfections are taken into account. In the latter case the restriction can be satisfied only approximately.

The "quality" of the control design is related to the sliding accuracy. It is worth mentioning that in practice, there are no design methods that can ideally maintain the desired constraint $s(x) = 0$. Therefore, there is a need to introduce some sort of comparison between different control systems. Further details and proofs can be found in [25].

Strictly speaking, any ideal sliding mode should be understood as the limit of movements when the imperfections disappear and the switching frequency tends to infinity. Therefore, if ε is taken as a measure of these imperfections, the accuracy of any sliding-mode control design can be characterised by its asymptotic behaviour as $\varepsilon \to 0$ [29].

For example, to obtain a real sliding mode of order r (with discrete switching), it is required to satisfy an order r of ideal sliding (at infinite switching frequency). So, most of the real second-order algorithms come from discretising ideal second-order algorithms [17, 29].

A special discrete switching algorithm that provides second-order real sliding was presented in [41]. Another example of a second-order real sliding controller is the "Drift Algorithm" [29]. Moreover, a real third-order sliding controller that only uses measures of s has been presented in [3].

3.4.4.2 HOSM Convergence Time

Prior to entering the section devoted to the design of specific Second-Order Sliding-Mode (SOSM) algorithms, a final general comment concerning the convergence time is of interest. Convergence in HOSM can be either asymptotic or in finite time. Examples of asymptotically stable sliding-mode algorithms of arbitrary order are well known in the literature [24]. On the other hand, fewer examples can be cited for r-*sliding* controllers that converge in finite time. For instance, these can be found for $r = 1$ (which is trivial), for $r = 2$ [2, 5, 29] and for $r = 3$ [24, 31]. Despite the fact that some arbitrary-order sliding-mode controllers of finite-time convergence have already been presented [33], its implementation is not yet widespread.

3.5 Design of Second-Order Sliding-Mode Controllers

3.5.1 Second-Order Sliding Generalised Problem

This final section is focused on the design of SISO second-order sliding-mode controllers, aiming to explain the specific algorithms that will be used in this book.

To this end, consider the uncertain nonlinear system (initially, not necessarily affine in the control), explicitly defined as

$$\begin{cases} \dot{x} = F(x, u, t) \\ s = s(x, t) \in \mathbb{R} \\ u = U(x, t) \in \mathbb{R} \end{cases} \tag{3.47}$$

with $x \in \mathbb{R}^n$, u the single control input, and F and s smooth functions. Note that in this section the possible direct dependence on t has been explicitly manifested in system (3.47), in order to better explain the subsequent SOSM design procedure.

As always, the ultimate control objective would be steering the sliding output s to zero. However, the SOSM approach enables not only that $s = 0$ and its time derivative $\dot{s} = 0$, but also finite time stabilisation of both, as long as s is of relative degree 1 or 2 with respect to the control input u. Moreover, in the former case the physical control action synthesised by the SOSM algorithm is continuous.

The SOSM design procedure depends on the bounds of certain functions that constitute the second time derivative of the sliding output s. Hence, as a first step, s is differentiated twice, and the following general expressions are derived:

$$\dot{s} = \frac{\partial}{\partial t} s(x, t) + \frac{\partial}{\partial x} s(x, t) F(x, u, t) \tag{3.48}$$

$$\ddot{s} = \frac{\partial}{\partial t} \dot{s}(x, t) + \frac{\partial}{\partial x} \dot{s}(x, t) F(x, u, t) + \frac{\partial}{\partial u} \dot{s}(x, t) \dot{u}(t) \tag{3.49}$$

Then, two different cases will be addressed, depending on the relative degree of s with respect to input u. Systems with relative degree 1 and relative degree 2 will be considered, respectively.

Case 1 Systems with relative degree 1.

In relative degree 1 systems, u appears in $\dot{s}$, thus in the expression of $\ddot{s}$ the derivative $\dot{u}$ is explicitly presented in affine form, as in (3.49). Therefore expression (3.49) can be given as follows:

$$\ddot{s} = \varphi(x, u, t) + \gamma(x, u, t) \dot{u}(t) \tag{3.50}$$

with $\varphi(x, u, t)$ and $\gamma(x, u, t)$ uncertain but uniformly bounded functions in a bounded domain. In order to specify the control problem, the following conditions must be assumed [29]:

1. There are bounds Γ_m and Γ_M such that within the region $|s(x,t)| < s_0$ the following inequality holds for all $t, x \in \mathscr{X}, u \in \mathscr{U}$:

$$0 < \Gamma_m \leq \gamma(x,u,t) = \frac{\partial}{\partial u}\dot{s}(x,t) \leq \Gamma_M \tag{3.51}$$

   The constant s_0 defines a region of operation around the sliding manifold, where the bounds are valid. Note that, eventually, an appropriate control action has to be included in the controller, in order to attract the system into this validity region.
2. There is also a bound Φ such that, within the region $|s(x,t)| < s_0$,

$$\left|\varphi(x,u,t) = \frac{\partial}{\partial t}\dot{s}(x,t) + \frac{\partial}{\partial x}\dot{s}(x,t).F(x,u,t)\right| \leq \Phi \tag{3.52}$$

for all $t, x \in \mathscr{X}, u \in \mathscr{U}$.

With these bounds at hand, the following differential inclusion can be proposed to replace (3.50) [33]:

$$\ddot{s} \in [-\Phi, \Phi] + [\Gamma_m, \Gamma_M]\dot{u} \tag{3.53}$$

This is a very important relation when considering robustness. As it will be demonstrated in the following subsection, many SOSM controllers ensure finite-time stabilisation of both $s(x,t) = 0$ and $\dot{s}(x,t) = 0$, not merely for the nominal original system, but for (3.53). Since inclusion (3.53) does not *remember* whether or not the original system (3.47) is perturbed (it will include both cases, as far as perturbations had been computed into the bounds), then such a controller will be obviously robust with respect to any perturbation or uncertainty existing in (3.47) and, consequently, translated to (3.50).

Case 2 Systems with relative degree 2.

In relative degree 2 systems, u is not present in $\dot{s}$, hence the derivative $\dot{u}$ does not appear in $\ddot{s}$ (i.e. the third term of (3.49) is null), resulting in

$$\ddot{s} = \frac{\partial}{\partial t}\dot{s}(x,t) + \frac{\partial}{\partial x}\dot{s}(x,t)F(x,u,t) \tag{3.54}$$

In this case, we will limit the analysis to affine in the control nonlinear systems of the form:

$$\dot{x} = F(x,u,t) = f(x,t) + g(x,t)u(t) \tag{3.55}$$

Therefore, expressions (3.54) and (3.55) can be combined as follows:

$$\ddot{s} = \varphi'(x,t) + \gamma'(x,t)u(t) \tag{3.56}$$

Once again $\varphi'(x,t)$ and $\gamma'(x,t)$ are uncertain but uniformly bounded functions in a bounded domain.

Fig. 3.6 System trajectory on the plane $(s, \dot{s})$

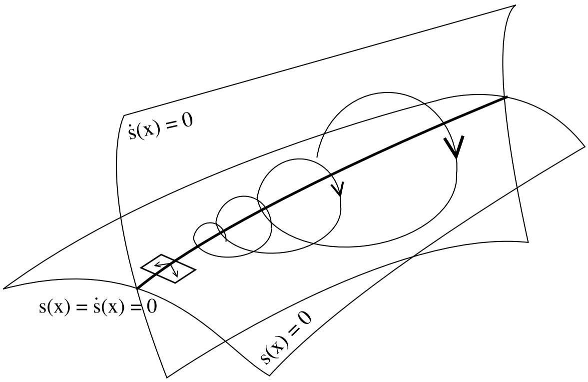

As in the relative degree 1 case, analogous conditions must be assumed:

1. There are bounds Γ'_m and Γ'_M such that, within the region $|s(x,t)| < s_0$, the following inequality holds for all $t, x \in \mathscr{X}, u \in \mathscr{U}$:

$$0 < \Gamma'_m \leq \gamma'(x,t) \leq \Gamma'_M \tag{3.57}$$

   and s_0 defines the region of validity around the sliding manifold.
2. There is also a bound Φ' such that, within the region $|s(x,t)| < s_0$,

$$\left|\varphi'(x,t)\right| \leq \Phi' \tag{3.58}$$

for all $t, x \in \mathscr{X}, u \in \mathscr{U}$.

In this case, the following differential inclusion can be proposed to replace (3.56):

$$\ddot{s} \in \left[-\Phi', \Phi'\right] + \left[\Gamma'_m, \Gamma'_M\right]u \tag{3.59}$$

Robustness considerations similar to the prior case can be established.

3.5.2 *Solution of the Control Problem. SOSM Algorithms*

There is a wide variety of proposals for second-order sliding-mode controllers that provide solutions to the aforementioned problem of finite-time convergence and robust stability. In this section three of the most widely-known algorithms will be reviewed. Two of them, the *Twisting* and *Sub-Optimal* algorithms, are devised for relative degree 2 systems, and the other one, the *Super Twisting* algorithm, is for relative degree 1 systems.

3.5.2.1 Twisting Algorithm

This is one of the first SOSM mode algorithms, and it is primarily intended for relative degree 2 systems. Once the initialisation phase is elapsed (i.e. the region

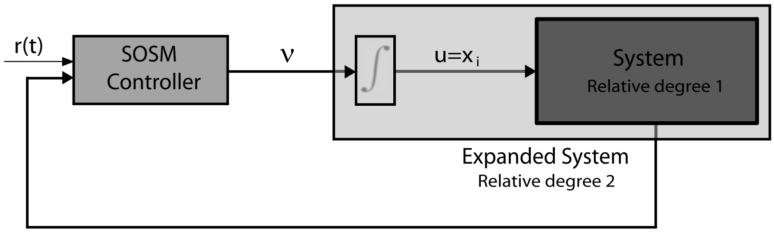

Fig. 3.7 Expanded system

$|s| < s_0$ is reached by using an appropriate extra control action), it generates system trajectories that encircle the origin of the plane $(s, \dot{s})$ an infinite number of times (Fig. 3.6), converging to it in finite time [29].

Consider system (3.47) under the conditions of Case 2 of Sect. 3.5.1; these are of relative degree 2 with respect to s and affine in the control form, as in (3.55). Additionally, the bounds defined in Case 2, conditions 1 and 2, exist and are available for the designer. Then, the *Twisting* algorithm can be written as

$$u = -r_1 \operatorname{sign}(s) - r_2 \operatorname{sign}(\dot{s}) \tag{3.60}$$

where r_1 and r_2 are the controller parameters, to be tuned based on the system bounds. It will be demonstrated in the sequel that if they simultaneously satisfy the conditions

$$\begin{gathered} r_1 > r_2 > 0 \\ \Gamma_m'(r_1 + r_2) - \Phi' > \Gamma_M'(r_1 - r_2) + \Phi' \\ \Gamma_m'(r_1 - r_2) > \Phi' \end{gathered} \tag{3.61}$$

then the *Twisting* controller (3.60) generates a second-order sliding mode that attracts the trajectories of the system to $s = \dot{s} = 0$ in finite time [25].

Twisting Adaptation to Relative Degree 1 Systems Prior to proving the convergence of the *Twisting* algorithm, it would be useful to explain how to apply it to relative degree 1 systems.

It is rather obvious that algorithms intended for relative degree 2 can straightforwardly be adapted for its implementation on relative degree 1 systems. The procedure would be as simple as to artificially increase the relative degree to 2 by expanding the system. To this end, an integrator is incorporated prior to input u, and a new artificial input ν is created (see Fig. 3.7) in accordance with the differential equation below:

$$\dot{u} = \nu(t) \tag{3.62}$$

Now, u has become a new internal state variable ($x_i = u$) of the following expanded system with artificial or auxiliary input ν:

$$\dot{x_e} = F_e(x_e, \nu, t) = f_e(x_e, t) + g_e(x_e, t)\nu(t) \tag{3.63}$$

with $x_e = [x^T \; x_i]^T \in \mathbb{R}^{n+1}$, ν the new input of the expanded system, and F_e, f_e and g_e smooth functions.

The expanded system (3.63) is then of relative degree 2 with respect to s and, consequently, fulfils the conditions required for the design of the *Twisting* algorithm. Following the steps previously described, a *Twisting* SOSM control signal would be synthesised for the relative degree 2 input:

$$\nu = \dot{u} = -r_1 \operatorname{sign}(s) - r_2 \operatorname{sign}(\dot{s}) \tag{3.64}$$

To conclude, it is pertinent to remark on the bounds required for the design. It is straightforward to infer, according with (3.56), that the expression of $\ddot{s}$ in terms of the expanded system becomes

$$\ddot{s} = \varphi'(x_e, t) + \gamma'(x_e, t)\nu(t) \tag{3.65}$$

In turn, if the expression of $\ddot{s}$ of the original system, i.e. the expression for relative degree 1 systems (3.50), is also written in terms of the expanded system variables, it results in

$$\begin{aligned} \ddot{s} &= \varphi(x, u = x_i, t) + \gamma(x, u = x_i, t)\dot{u}(t) \\ &= \varphi(x, x_i, t) + \gamma(x, x_i, t)\nu(t) \end{aligned} \tag{3.66}$$

Comparing (3.65) and (3.66), it can be appreciated that in this case, in which the relative degree 2 system comes from an artificially expanded relative degree 1 system, the functions to be bounded are exactly the same to those of the latter (i.e. $\varphi'(x_e, t) = \varphi(x, u, t)$ and $\gamma'(x_e, t) = \gamma(x, u, t)$). So, in this particular case, this would allow the use of the same bounds for designing either relative degree 1 or 2 SOSM controllers. In this way, the computations involved in the design procedure of this type of systems are significantly alleviated.

Proof of Convergence of the Twisting Algorithm Auxiliary System To analyse the convergence of the algorithm, consider a suitable auxiliary system, namely a double integrator $\ddot{s} = u$. This system has been chosen given that it will behave as a "majorant" of the system under consideration (3.56), i.e. it will give the worst case for the region of convergence in the phase plane $(s, \dot{s})$. Then, controlling the auxiliary system with a control law of the *Twisting* form $u = -b_1 \operatorname{sign}(s) - b_2 \operatorname{sign}(\dot{s})$, yields

$$\ddot{s} = \frac{d\dot{s}}{dt} = \frac{d\dot{s}}{ds}\dot{s} = -b_1 \operatorname{sign}(s) - b_2 \operatorname{sign}(\dot{s}) \tag{3.67}$$

with constant parameters b_1 and b_2 satisfying $b_1 > b_2 > 0$.

Now, the task in this first stage will be to show that the solutions of (3.67) converge to the origin ($\dot{s} = s = 0$) in finite time. This result will be used at the end of the subsection to prove the convergence of the uncertain system under study.

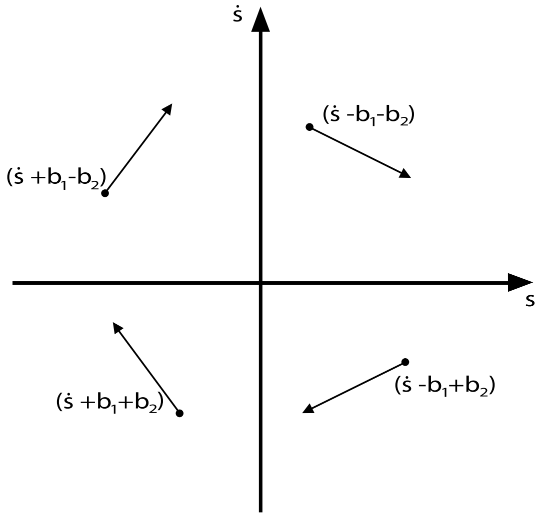

Fig. 3.8 Vector field

Analysing the differential equation it can be noticed that

$$\frac{d\dot{s}}{ds} = \begin{cases} \frac{-b_1-b_2}{\dot{s}} & \text{if } s > 0,\ \dot{s} > 0 \\ \frac{-b_1+b_2}{\dot{s}} & \text{if } s > 0,\ \dot{s} < 0 \\ \frac{b_1-b_2}{\dot{s}} & \text{if } s < 0,\ \dot{s} > 0 \\ \frac{b_1+b_2}{\dot{s}} & \text{if } s < 0,\ \dot{s} < 0 \end{cases} \tag{3.68}$$

Then, the system vector field will take the shape shown in Fig. 3.8.

Taking the initial conditions $P_1 = (0, \dot{s}_0)$, the solution of (3.67) for the first quadrant can be found as follows:

$$\int_0^{\dot{s}} \dot{s} d\dot{s} = \int_{s_1}^{s} -(b_1 + b_2) ds \tag{3.69}$$

$$\frac{1}{2}\dot{s}^2 = (b_1 + b_2)(s_1 - s) \tag{3.70}$$

$$\Rightarrow \quad s = s_1 - \frac{\dot{s}^2}{2(b_1 + b_2)} \tag{3.71}$$

For the second quadrant, a similar expression can be found:

$$s = s_1 - \frac{\dot{s}^2}{2(b_1 - b_2)} \tag{3.72}$$

Taking two fixed points of this trajectory, $P_1 = (0, \dot{s}_0)$ and $P_2 = (0, \dot{s}_1)$ (see Fig. 3.9), it can be concluded that

$$\begin{aligned} \dot{s}_0^2 &= s_1 2(b_1 + b_2) \\ \dot{s}_1^2 &= s_1 2(b_1 - b_2) \end{aligned} \tag{3.73}$$

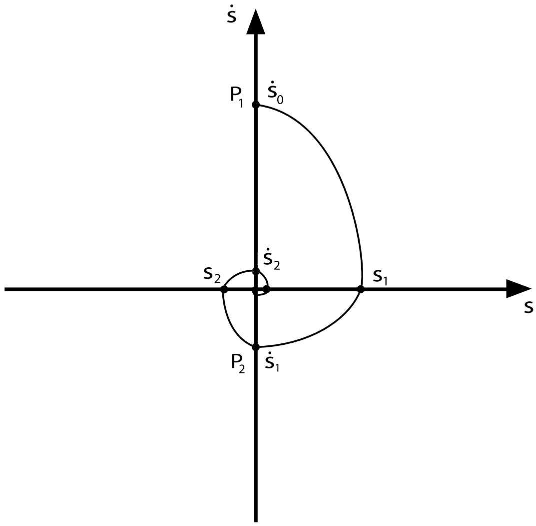

Fig. 3.9 Phase trajectory of the *Twisting* algorithm

$$\Rightarrow \quad \frac{|\dot{s}_1|}{|\dot{s}_0|} = \sqrt{\frac{b_1 - b_2}{b_1 + b_2}} = q < 1 \tag{3.74}$$

Extending this reasoning to the rest of the trajectory, it is verified that the following inequality always holds:

$$\frac{|\dot{s}_{i+1}|}{|\dot{s}_i|} = q < 1 \tag{3.75}$$

Therefore, the algorithm converges to the origin.

Time of Convergence Considering t_1^+ as the time that takes the auxiliary system trajectories to go from the point $\dot{s}_0$ to s_1. Integrating Eq. (3.67) in the first quadrant, it results in

$$\int_{\dot{s}_0}^{\dot{s}} d\dot{s} = \int_0^t -(b_1 + b_2)dt \tag{3.76}$$

$$\Rightarrow \quad \dot{s}(t) = -(b_1 + b_2)t + \dot{s}_0 \tag{3.77}$$

Knowing that $\dot{s}(t_1^+) = 0$, we get that

$$t_1^+ = \frac{\dot{s}_0}{b_1 + b_2} \tag{3.78}$$

The computation of t_1^- (time that takes the system to go from s_1 to $\dot{s}_1$) is similar to the previous step:

$$\dot{s}(t) = s_1 - \frac{\dot{s}^2}{2(b_1 - b_2)} = s_1 - \frac{[-(b_1 - b_2)t]^2}{2(b_1 - b_2)} = s_1 - \frac{(b_1 - b_2)t^2}{2} \tag{3.79}$$

Taking into account that $s(t_1^-) = 0$ and using (3.73), we can state that

$$t_1^- = \sqrt{\frac{2s_1}{b_1 - b_2}} = \sqrt{\frac{1}{(b_1 - b_2)(b_1 + b_2)}}\dot{s}_0 \tag{3.80}$$

This means that the time interval t_1 of the trajectory $\dot{s}_0 s_1 \dot{s}_1$ is

$$t = t_1^+ + t_1^- = \eta \dot{s}_0 \tag{3.81}$$

where

$$\eta = \frac{1}{b_1 + b_2} + \sqrt{\frac{1}{(b_1 - b_2)(b_1 + b_2)}} \tag{3.82}$$

More generally, we can state that

$$t_i = \eta |\dot{s}_{i-1}| = \eta q^{i-1} \dot{s}_0 \tag{3.83}$$

So the total convergence time of the auxiliary system is given by

$$T = \sum_{i=1}^{\infty} t_i = \sum_{i=1}^{\infty} \eta |\dot{s}_{i-1}| = \sum_{i=1}^{\infty} \eta q^{i-1} \dot{s}_0 = \frac{\eta \dot{s}_0}{1-q} \tag{3.84}$$

In the sequel, it will be demonstrated that, with an adequate selection of b_1 and b_2, the auxiliary system effectively acts as a majorant of (3.56) and (3.84) is a bound for its convergence time.

Convergence of the Uncertain System Once the convergence of the auxiliary system has been demonstrated, the last stage consists of using this result to prove the convergence of the relative degree 2 uncertain system under study.

To this end, reconsider the differential equation

$$\ddot{s} = \varphi'(x,t) + \gamma'(x,t)u \tag{3.85}$$

with the aforementioned bounds

$$\left|\varphi'(x,t)\right| \le \Phi', \quad 0 \le \Gamma'_m \le \gamma'(x,t) \le \Gamma'_M \tag{3.86}$$

and the differential inclusion

$$\ddot{s} \in \left[-\Phi', \Phi'\right] + \left[\Gamma'_m, \Gamma'_M\right]u \tag{3.87}$$

provided that the solutions of (3.85) are understood in the Filippov sense.

The *Twisting* law (3.60) with r_1 and r_2 simultaneously satisfying

$$\begin{gathered} r_1 > r_2 > 0 \\ \Gamma'_m(r_1 + r_2) - \Phi' > \Gamma'_M(r_1 - r_2) + \Phi' \\ \Gamma'_m(r_1 - r_2) > \Phi' \end{gathered} \tag{3.88}$$

is used to control the system.

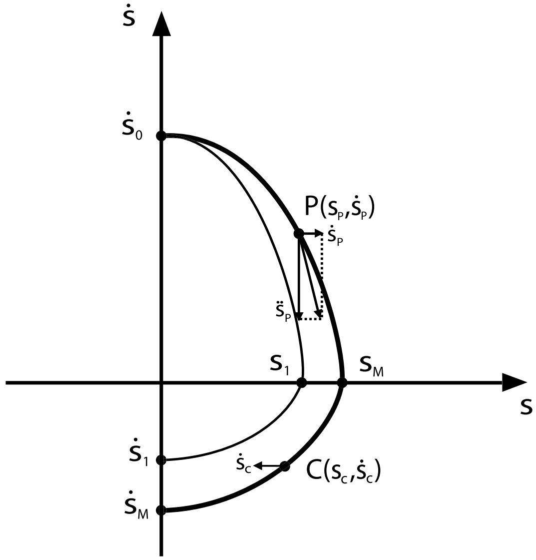

Fig. 3.10 *Twisting* algorithm and majorant trajectories

Then, to prove that the auxiliary system (3.67) is a majorant for (3.85) controlled with the *Twisting* algorithm, the following appropriate selection for constants $b_1 > b_2 > 0$ is proposed:

$$b_1 + b_2 = \Gamma'_m(r_1 + r_2) - \Phi', \qquad b_1 - b_2 = \Gamma'_M(r_1 - r_2) + \Phi' \tag{3.89}$$

With this parameter selection, trajectories $\dot{s}_0 s_1 \dot{s}_1$ and $\dot{s}_0 s_M \dot{s}_M$ in Fig. 3.10 correspond to (3.85) and (3.67), respectively, with common initial conditions $s = 0$ and $\dot{s} = \dot{s}_0 > 0$ for $t = 0$.

In particular, $\dot{s}_0 s_M \dot{s}_M$ is the so-called "majorant curve" of the system. One of its points, $P(s_p, \dot{s}_p)$, in the first quadrant is considered. If the trajectories of the system (3.85) pass through this point, controlled by (3.60), the system velocity would have the coordinates $(\dot{s}_p, \ddot{s}_p)$. Note that the horizontal component of velocity $(\dot{s}_p)$ is the y-coordinate of the point P (positive value).

On the other hand, using the control (3.60) in system (3.87) on the first quadrant, the following will be fulfilled:

$$\ddot{s} \in \left[-\Phi', \Phi'\right] + \left[\Gamma'_m(-r_1 - r_2), \Gamma'_M(-r_1 - r_2)\right] \tag{3.90}$$

Moreover, due to the fact that inequalities (3.88) hold, the vertical component is kept within the following limits:

$$-\Phi' - \Gamma'_M(r_1 + r_2) \le \ddot{s} \le \Phi' - \Gamma'_m(r_1 + r_2) < 0 \tag{3.91}$$

This implies that the velocity of system (3.85), (3.60) at $P(s_p \dot{s}_p)$, will always "point" to the interior of the region bounded by the axes $s = 0$, $\dot{s} = 0$ and the surrounding curve (3.67), (3.89). Then, the trajectory of system (3.85), (3.60) intersects the axis $\dot{s} = 0$ in a point $s_1 \le s_M$ in finite time $t_1^+ \le t_M^+$.

Considering the trajectories $s_1\dot{s}_1$ and $s_M\dot{s}_M$ of systems (3.85), (3.60) and (3.67) in the second quadrant ($s \geq 0$, $\dot{s} \leq 0$), a point $C(s_C, \dot{s}_C)$ where similar properties are verified can be taken. As it can be inferred from inequality (3.88), in this quadrant the module of the vertical component of velocity vector (3.85), (3.60) is smaller than the surrounding system (3.67), while the horizontal component is $\dot{s}_C$:

$$-\Phi' - \Gamma'_M(r_1 - r_2) \leq \ddot{s} \leq \Phi' - \Gamma'_m(r_1 - r_2) < 0 \tag{3.92}$$

This means that the trajectories of system (3.85), (3.60) are inside the surrounding system. On the other hand, the time required to cover the vertical segment $(0, \dot{s}_1)$ is the same, but the surrounding trajectory must also cover the vertical segment $\dot{s}_1, \dot{s}_M$. This is the reason why $t_1^- \leq t_M^-$, where t_1^- is the time it takes the system to cover the trajectory $s_1\dot{s}_1$, and t_M^- is that for $s_M\dot{s}_M$.

Then, the trajectory of system (3.85), (3.60) intersects $s = 0$ at $\dot{s}_1$. Moreover, $|\dot{s}_1| \leq |\dot{s}_M|$, and therefore the evolution time of the uncertain system is bounded by the majorant as $t_1 \leq t_M$.

3.5.2.2 Super Twisting Algorithm

The *Super Twisting* algorithm, one of the most widely used algorithms of the family, is particularly intended for systems with relative degree 1 [25, 29]. Highly suitable for real implementation, with a proper choice of parameters, this algorithm converges in finite time after describing a trajectory similar to the one of the *Twisting* algorithm (Fig. 3.11). The most distinctive features of the *Super Twisting* algorithm are the aforementioned direct applicability to relative degree 1 systems, the synthesis of continuous control actions and the absence of a measurement of $\dot{s}$ in the control law. This makes it more immune to output measurement noise and possible errors in the estimation of $\dot{s}$.

The control action $u(t)$ of the *Super Twisting* algorithm is composed of two continuous terms, even though the first one is given by the integral of a discontinuous action. Once the validity region $|s| < s_0$ is attained, with the help of an appropriate reaching control action, the *Super Twisting* control is given by

$$u(t) = u_1(t) + u_2(t) \tag{3.93}$$

with

$$\begin{aligned} \dot{u}_1(t) &= -\alpha\,\mathrm{sign}(s) \\ u_2(t) &= -\lambda|s|^\rho\,\mathrm{sign}(s) \end{aligned} \tag{3.94}$$

where $\alpha > 0$, $\lambda > 0$ and $\rho \in (0, 1/2]$ are the parameters of the controller. The restrictions for their design are based on the bounds defined in Case 1 and conditions 1 and 2 in Sect. 3.5.1. The following are sufficient conditions for convergence in finite

Fig. 3.11 Phase trajectory of the *Super Twisting* algorithm

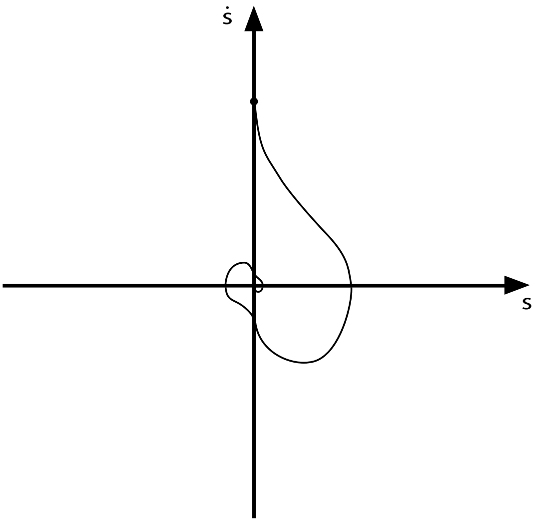

time to the sliding manifold [25, 29]:

$$\begin{aligned} &\alpha > \frac{\Phi}{\Gamma_m} \\ &\lambda^2 > \frac{2}{\Gamma_m^2} \frac{(\Gamma_m \alpha + \Phi)^2}{(\Gamma_m \alpha - \Phi)} \quad \text{if } \rho = 0.5 \end{aligned} \tag{3.95}$$

Note that if $\rho = 1$ and α and λ/α are large enough, it can be even proven that there will be a stable second-order sliding mode. In this case, $|s| + |\dot{s}|$ would tend to zero with exponential upper and lower bounds.

Super Twisting Adaptation to Relative Degree 2 Systems In similar way that an algorithm intended for relative degree 2 can be adapted for its implementation on relative degree 1 systems, the Super Twisting algorithm can be adapted for application to relative degree 2 systems. In this case a differentiator should be incorporated into the system. This is not at all a specific subject matter of this book, and therefore it will not be addressed here. Nevertheless, to give an idea of the procedure, consider that the artificial input ν is created in this case such that $u = \dot{\nu}$, i.e. differentiating the new input instead of integrating it (as it was done in the Twisting analogous case). Then, substituting $\dot{\nu}$ for u in the expression of $\ddot{s}$ for the relative degree 2 system (3.55), it would become affine with respect to the derivative of the input, specifically, the artificial input ν. Displaying that form, the differential inclusion proposed for relative degree 1 is applicable to (3.56), hence the standard Super Twisting algorithm could be used to synthesise the control signal for the artificial input ν. The actual implementation method and the proper use of differentiators are much more elaborate and, as previously stated, far exceed the scope of this book. The interested reader is strongly encouraged to read the specialised literature on this topic (e.g., [4, 32]).

Proof of Convergence of the Super Twisting Algorithm Consider now the controlled process (3.47) with output s of relative degree 1 with respect to u. As was said, if the control problem satisfies conditions (3.51), (3.52), the system solutions can be understood in the sense of Filippov, and Eq. (3.50) can be replaced by the differential inclusion (3.53).

Then, substituting (3.94) into the differential inclusion (3.53), the overall system performance and the majorant curves that limit the evolution of the system trajectories can be evaluated. Consider the case where $|s| < |s_0|$ and the trajectory of the system is within the first quadrant ($s > 0$ and $\dot{s} > 0$):

$$\ddot{s} \in [-\Phi, \Phi] + [\Gamma_m, \Gamma_M]\big(-\lambda\rho s^{\rho-1}\dot{s} - \alpha\big) \tag{3.96}$$

Due to the fact that in this quadrant $\dot{s} > 0$, in order to decrease the value of $\dot{s}$ and ensure that the system trajectories cross $\dot{s} = 0$, the condition $\ddot{s} < 0$ must be achieved in the entire quadrant. The worst possible scenario is when $\varphi(x,t) = \Phi$ (maximum positive value that the vector field φ can take) and $\gamma(x,t) = \Gamma_m$ (lower dominance of control in the system dynamics):

$$\ddot{s} = \Phi + \Gamma_m\big(-\lambda\rho s^{\rho-1}\dot{s} - \alpha\big) < 0 \tag{3.97}$$

To keep the sign of $\ddot{s}$ negative, even when $\lambda\rho s^{\rho-1}\dot{s} \to 0$, the relation $\Phi - \Gamma_m\alpha < 0$ must be satisfied. This imposes the first convergence condition of the algorithm:

$$\alpha > \frac{\Phi}{\Gamma_m} \tag{3.98}$$

To improve clarity in the analysis, the second convergence condition of the algorithm will be obtained with the help of the following change of notation: $s = z_1$ and $\dot{s} = z_2$. Then, the dynamics of the planar system in the first quadrant is given by

$$\begin{cases} \dot{z}_1 = z_2 \\ \dot{z}_2 = \varphi + \gamma\big(-\lambda\rho z_1^{\rho-1} z_2 - \alpha\big) \end{cases} \tag{3.99}$$

Considering the worst-case scenario for this quadrant ($\varphi = \Phi$ and $\gamma = \Gamma_m$), system (3.99) will have a limit trajectory in the solutions of the following planar system:

$$\begin{cases} \dot{z}_1 = z_2 \\ \dot{z}_2 = \Phi + \Gamma_m\big(\lambda\rho(-z_1)^{\rho-1} z_2 + \alpha\big) \end{cases} \tag{3.100}$$

The analytical solutions of this nonlinear system cannot be straightforwardly found, but numeric tools can be used to predict the solution from an initial condition. Figure 3.12 presents the results of a numerical evaluation of the limit trajectories of system (3.99) with a set of parameters arbitrarily chosen as an example ($\Phi = 10$, $\Gamma_m = 1$, $\Gamma_M = 1.7$, $\alpha = 50$, $\lambda = 15$ and $\rho = 0.5$).

The case of slower decrease of $\ddot{s}$ takes place as $\lambda\rho s^{\rho-1}\dot{s} \to 0$. Thus, in the first quadrant, the majorant curve is governed by the following expression:

$$\ddot{s} = \Phi - \Gamma_m\alpha \tag{3.101}$$

Integrating successively this equation, the following general expression with initial conditions $(0, \dot{s}_0)$ can be found, which represent the majorant curve of the sys-

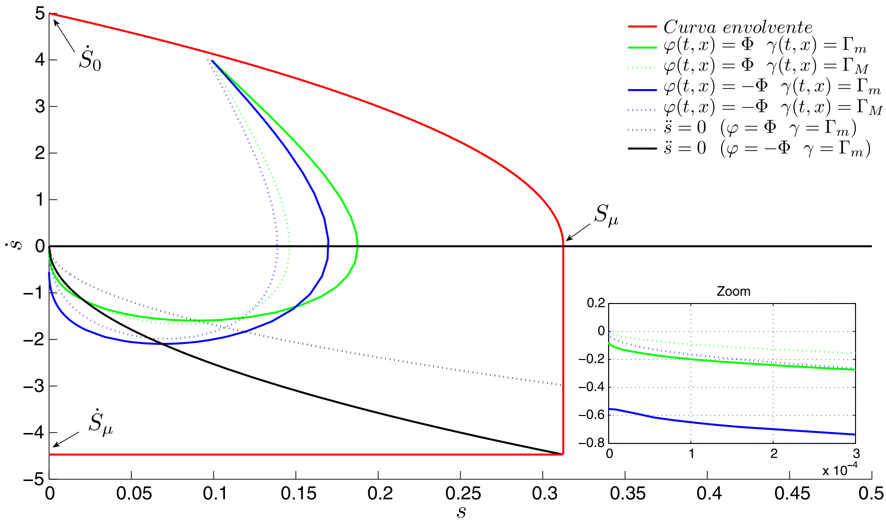

Fig. 3.12 Example of convergence of the *Super Twisting* algorithm

tem trajectories in the first quadrant:

$$s = (\dot{s} - \dot{s}_0)^2 \frac{1}{2K} + (\dot{s} - \dot{s}_0)\frac{\dot{s}_0}{K} \tag{3.102}$$

with

$$K = \Phi - \Gamma_m \alpha < 0 \tag{3.103}$$

In the example of Fig. 3.12, the external line shows the majorant curve of the system trajectories (3.99), with the corresponding parameters listed above. It is important to note that, although the trajectories can be closer to the majorant curve at certain points, the majorant curve does not represent a possible path of the system, which would imply $\lambda \rho s^{\rho-1}\dot{s} = 0$ for all $(s, \dot{s})$.

Using an analogous analysis on the fourth quadrant, similar equations for the system dynamics can be found:

$$\begin{cases} \dot{z}_1 = z_2 \\ \dot{z}_2 = \varphi + \gamma\left(\lambda\rho(-z_1)^{\rho-1} z_2 + \alpha\right) \end{cases} \tag{3.104}$$

In this case, there are no restrictions on the sign of $\ddot{s}$, but it can be known from the continuity of trajectories that, in the first section, $\ddot{s} < 0$. Then, from an isocline analysis, the area where $\ddot{s}$ is zero can be determined. Taking $\ddot{s} = 0$ in the worst-case scenario of the quadrant ($\varphi = -\Phi$ and $\gamma = \Gamma_m$), we obtain that

$$\dot{s} = -\beta s^{1-\rho} \tag{3.105}$$

with

$$\beta = \frac{\Phi + \Gamma_m \alpha}{\Gamma_m \lambda \rho} \tag{3.106}$$

Therefore, when crossing the curve (3.105), (3.106), the system trajectories will do it with $\ddot{s} = 0$, yielding a local minimum at $\dot{s}$ and a change of sign in $\ddot{s}$ (see Fig. 3.12). Since in this quadrant $\dot{s} < 0$, the function $s(x)$ decreases monotonically. This ensures an intersection point with the curve (3.105), (3.106). To define a majorant curve of the system, the minimum possible value of $\dot{s}$ can be analysed, which is determined by the value taken by (3.105), (3.106) when $s = s_\mu$ (see Fig. 3.12):

$$\dot{s}_\mu = -\beta s_\mu^{1-\rho} = -\frac{\Phi + \Gamma_m\alpha}{\Gamma_m\lambda\rho}\left(-\frac{\dot{s}_0^2}{2(\Phi - \Gamma_m\alpha)}\right)^{1-\rho} \tag{3.107}$$

Finally, to ensure the algorithm convergence to the origin, it is necessary to satisfy that $|\dot{s}_\mu| < |\dot{s}_0|$:

$$\frac{|\dot{s}_\mu|}{|\dot{s}_0|} = \frac{\Phi + \Gamma_m\alpha}{\Gamma_m\lambda\rho}\left(\frac{\dot{s}_0^2}{2(\Gamma_m\alpha - \Phi)}\right)^{1-\rho}\frac{1}{\dot{s}_0} < 1 \tag{3.108}$$

If $\rho = 0.5$, this condition is reduced to

$$\lambda^2 \geq \frac{2}{\Gamma_m^2}\frac{(\Gamma_m\alpha + \Phi)^2}{(\Gamma_m\alpha - \Phi)} \tag{3.109}$$

For the case where $|s| > s_0$, a simplified expression similar to (3.102) can be found, which ensures that the controlled system trajectories arrive at the area $|s| < s_0$ in finite time.

3.5.2.3 Sub-Optimal Algorithm

Similarly to the *Twisting* algorithm, this SOSM controller is primarily intended for relative degree 2 systems. It was developed as a Sub-Optimal feedback implementation of the classical time-optimal control for the uncertain double integrator problem [2].

In this case, the system trajectories on the plane $(s, \dot{s})$ are confined within limit parabolic arcs that include the origin. So both twisting and leaping behaviours are possible. A most important feature is that the coordinates of the successive trajectory intersection with axis s decrease in geometric progression (see Fig. 3.13).

Given that the *Sub-Optimal* algorithm is a controller primarily intended for relative degree 2 systems, we consider similar conditions to the ones established for *Twisting* algorithm (i.e., conditions of Case 2 of Sect. 3.5.1). Then, once the region of validity is reached, the *Sub-Optimal* algorithm is defined by the following control law:

$$\begin{aligned} u &= -\alpha(t)U\,\mathrm{sign}(s - \beta s_M) \\ \alpha(t) &= \begin{cases} 1 & \text{if } (s - \beta s_M)s_M \geq 0 \\ \alpha^* & \text{if } (s - \beta s_M)s_M < 0 \end{cases} \end{aligned} \tag{3.110}$$

where $\alpha^* > 1$ is the so-called modulation factor, $0 \leq \beta < 1$ is the anticipation factor, and $U > 0$ is the minimum control magnitude. s_M corresponds to the last singular

Fig. 3.13 Phase trajectory of the *Sub-Optimal* algorithm

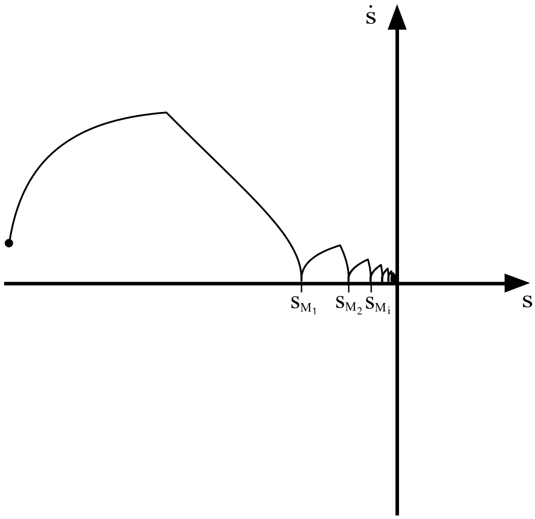

value of the function s, i.e. the last value of s at the time its derivative $\dot{s}$ reaches zero (see Fig. 3.13). This value must be refreshed every time $\dot{s}$ zeroes, thus the *Sub-Optimal* algorithm is particularly suitable for plants that incorporate a special device or software code to detect the singular values (s_M) (i.e. peak detector).

The parameters of the controller, α^*, β and U, should be tuned based on the bounds defined in conditions 1 and 2 of Case 2, Sect. 3.5.1. The sufficient conditions for the finite-time convergence and robust stabilisation of the system are

$$\begin{aligned} &U > \frac{\Phi'}{\Gamma'_m} \\ &\alpha^* \in [1; +\infty) \cap \left[\frac{\Phi' + (1-\beta)\Gamma'_M U}{\beta \Gamma'_m U}; +\infty \right) \end{aligned} \tag{3.111}$$

which are known as the dominance condition and the convergence condition, respectively. The former ensures that the control has sufficient authority to affect the sign of $\ddot{s}$. The latter guarantees the sliding-mode stability and determines the rate of convergence. A detailed analysis and proof of convergence can be found in [2] and [5].

Sub-Optimal Algorithm Adaptation to Relative Degree 1 Systems Similarly to the *Twisting* algorithm case, the application of the *Sub-Optimal* algorithm to relative degree 1 systems can be achieved by artificially increasing the relative degree, with the incorporation of an integrator prior to the system input u. The procedure to be followed is exactly the same as that described in the *Twisting* algorithm Sect. 3.5.2.1.

3.6 Conclusions

Fundamentals of sliding-mode control have been introduced in this chapter. This control theory has proven to be capable of successfully dealing with nonlinear systems, presenting several attractive characteristics. Among them, finite convergence, system order reduction and robustness against certain disturbances are the most relevant. In this context, the extension known as Higher-Order Sliding Modes adds chattering reduction to the list of positive features, improving accuracy in realisation and, in several plants, contributing to extending the service life of the actuators. These, together with relatively low on-line computational cost, make the HOSM technique specially suitable for implementation.

To this end, several algorithms have been developed, particularly the Second-Order Sliding-Mode ones. In this chapter, three of the most widely used SOSM controllers have been reviewed, namely *Twisting*, *Super Twisting* and *Sub-Optimal*. There are many others that robustly solve the problem of convergence, each one with its own advantages and features (e.g., *Drift algorithm* [18, 29], *Global algorithm* [5] and *Prescribed convergence law algorithm* [29]).

Then, the challenge now is to tackle the specific problem of PEM fuel cell control and assess the applicability of this control technique, with the objective of enhancing fuel cell efficiency and increasing their service life. This will be the topic of the next chapter.

References

1. Barbot JP, Perruquetti W (eds) (2002) Sliding mode control in engineering. Dekker, New York
2. Bartolini G, Ferrara A, Usai E (1998) Chattering avoidance by second order sliding mode control. IEEE Trans Autom Control 43(2):241–246
3. Bartolini G, Levant A, Pisano A, Usai E (1999) 2-Sliding mode with adaptation. In: Proceedings of the 7th IEEE Mediterranean conference on control and systems, Haifa, Israel
4. Bartolini G, Levant A, Pisano A, Usai E (2002) Higher-order sliding modes for output-feedback control of nonlinear uncertain systems. In: Variable structure systems: towards the 21st century. Lecture notes in control and information sciences, vol 274, Springer, Berlin, pp 83–108 (Chap 6)
5. Bartolini G, Pisano A, Punta E, Usai E (2003) A survey of applications of second-order sliding mode control to mechanical systems. Int J Control 76(9/10):875–892
6. Bartolini G, Fridman L, Pisano A, Usai E (eds) (2008) Modern sliding mode control theory. New perspectives and applications. Lecture notes in control and information sciences, vol 375. Springer, Berlin
7. Boiko I, Fridman L (2005) Analysis of chattering in continuous sliding mode controllers. IEEE Trans Autom Control 50(9):1442–1446
8. Boiko I, Fridman L, Pisano A, Usai E (2007) Analysis of chattering in systems with second-order sliding modes. IEEE Trans Autom Control 52(11):2085–2102
9. Bondarev A, Bondare S, Kostyleva N, Utkin V (1985) Sliding modes in systems with asymptotic state observers. Autom Remote Control 46(5):679–684
10. Burton J, Zinober A (1986) Continuous approximation of variable structure control. Int J Syst Sci 17:875–885

11. Cortes J (2008) Discontinuous dynamical systems—a tutorial on solutions, nonsmooth analysis, and stability. IEEE Control Syst Mag 28(3):36–73
12. DeCarlo R, Zak S, Matthews G (1988) Variable structure control of nonlinear multivariable systems: a tutorial. Proc IEEE 76(3):212–232
13. Drazenovic B (1969) The invariance conditions in variable structure systems. Automatica 5:286–295
14. Edwards C, Spurgeon S (1998) Sliding mode control: theory and applications, systems and control book series. Taylor & Francis, London
15. Edwards C, Fossas Colet E, Fridman L (eds) (2006) Advances in variable structure and sliding mode control. Lecture notes in control and information sciences, vol 334. Springer, Berlin
16. Emelyanov S (1957) Variable structure control systems. Nauka, Moscow
17. Emelyanov S, Korovin S (1981) Applying the principle of control by deviation to extend the set of possible feedback types. Sov Phys Dokl 26(6):562–564
18. Emelyanov S, Korovin S, Levantovsky L (1986) Higher order sliding regimes in the binary control systems. Sov Phys Dokl 31(4):291–293
19. Filippov A (1960) Differential equations with discontinuous right-hand side. Mat Sb (in Russian). English translation: Trans. Am Math. Soc. 62 (1964)
20. Filippov A (1988) Differential equations with discontinuous righthand sides. Mathematics and its application. Kluwer Academic, Dordrecht
21. Floquet T, Barbot J-P, Perruquetti W (2003) Higher-order sliding mode stabilization for a class of nonholonomic perturbed systems. Automatica 39(6):1077–1083
22. Fridman L (2001) An averaging approach to chattering. IEEE Trans Autom Control 46(8):1260–1265
23. Fridman L (2003) Chattering analysis in sliding mode systems with inertial sensors. Int J Control 76(9/10):906–912
24. Fridman L, Levant A (1996) Higher order sliding modes as a natural phenomenon in control theory. In: Robust control via variable structure and Lyapunov techniques. Lecture notes in control and information sciences, vol 217. Springer, London, pp 106–133 (Chap 7)
25. Fridman L, Levant A (2002) Higher order sliding modes. In: Sliding mode control in engineering. Dekker, New York, pp 53–101 (Chap 3)
26. Hung JY, Gao W, Hung JC (1993) Variable structure control: a survey. IEEE Trans Ind Electron 40(1):2–22
27. Isidori A (1995) Nonlinear control systems. Springer, Berlin
28. Khalil H (2002) Nonlinear systems, 3rd edn. Prentice Hall, New York
29. Levant A (1993) Sliding order and sliding accuracy in sliding mode control. Int J Control 58(6):1247–1263
30. Levant A (1998) Arbitrary-order sliding modes with finite time convergence. In: Proceedings of the 6th IEEE Mediterranean conference on control and systems, Alghero, Sardinia, Italy.
31. Levant A (2001) Universal SISO sliding-mode controllers with finite-time convergence. IEEE Trans Autom Control 46(9):1447–1451
32. Levant A (2003) Higher order sliding modes, differentiation and output feedback control. Int J Control 76(9):924–941
33. Levant A (2005) Homogeneity approach to high-order sliding mode design. Automatica 41:823–830
34. Levant A (2007) Construction principles of 2-sliding mode design. Automatica 43(4):576–586
35. Plestan F, Glumineau A, Laghrouche S (2008) A new algorithm for high order sliding mode control. Int J Robust Nonlinear Control 18(4–5):441–453
36. Sabanovic A, Fridman L, Spurgeon S (eds) (2004) Variable structure systems: from principles to implementation. IET control engineering series. IET, London
37. Shtessel Y, Shkolnikov I, Brown M (2003) An asymptotic second-order smooth sliding mode control. Asian J Control 5:498–503
38. Sira-Ramirez H (1988) Differential geometric methods in variable structure control. Int J Control 48(5):1359–1390

39. Slotine J (1991) Applied nonlinear control. Prentice Hall, New York
40. Sontag E (1998) Mathematical control theory: deterministic finite dimensional systems. Springer, Berlin
41. Su W, Drakunov S, Ozguner U (1994) Implementation of variable structure control for sampled-data systems. In: Proceedings of IEEE workshop on robust control via variable structure and Lyapunov techniques, Benevento, Italy, pp 166–173
42. Utkin V (1978) Sliding modes and their application in variable structure systems. Mir, Moscow
43. Utkin V (2002) First stage of VSS: people and events. Springer, Berlin, pp 1–33 (Chap 1)
44. Utkin V, Gulder J, Shi J (1999) Sliding mode control in electro mechanical systems. Taylor & Francis, London
45. Young K, Utkin V, Ozguner U (1999) A control engineer's guide to sliding mode control. IEEE Trans Control Syst Technol 7(3):328–342
46. Yu X, Xu JX (eds) (2002) Variable structure systems: towards the 21st century. Springer, Berlin